Eur. Phys. J. C 48, 207–213 (2006)
Digital Object Identifier (DOI) 10.1140/epjc/s2006-02613-8

THE EUROPEAN PHYSICAL JOURNAL C

J/ψ gluonic dissociation revisited: III. Effects of transverse hydrodynamic flow

B.K. Patra[1,a], V.J. Menon[2]

[1] Department of Physics, Indian Institute of Technology, Roorkee 247 667, India
[2] Department of Physics, Banaras Hindu University, Varanasi 221 005, India

Received: 9 January 2006 / Revised version: 11 May 2006 /
Published online: 16 August 2006 – © Springer-Verlag / Società Italiana di Fisica 2006

Abstract. In a recent paper [B.K. Patra, V.J. Menon, Eur. Phys. J. C **44**, 567 (2005)] we developed a very general formulation to take into account explicitly the effects of the hydrodynamic flow profile on the gluonic breakup of J/ψs produced in an equilibrating quark–gluon plasma. Here we apply that formulation to the case when the medium is undergoing a cylindrically symmetric *transverse* expansion starting from RHIC or LHC initial conditions. Our algebraic and numerical estimates demonstrate that the transverse expansion causes enhancement of the local gluon number density n_g, affects the p_{T}-dependence of the average dissociation rate $\langle\tilde{\Gamma}\rangle$ through a partial-wave interference mechanism and makes the survival probability $S(p_{\mathrm{T}})$ to change with p_{T} very slowly. Compared to the previous case of a longitudinal expansion the new graph of $S(p_{\mathrm{T}})$ is pushed up at LHC but develops a rich structure at RHIC, due to a competition between the transverse catch-up time and the plasma lifetime.

PACS. 12.38.Mh

1 Introduction

It is a well-recognized fact that a hydrodynamic expansion can significantly influence the internal dynamics of, and signals coming from, the parton plasma produced in relativistic heavy-ion collisions. The scenario of J/ψ suppression due to gluonic bombardment [1–8] now becomes very nontrivial because of two reasons:

i) the flow causes inhomogeneities with respect to the time-space location x and
ii) careful Lorentz transformations must be carried out among the rest frames of the fireball, the medium, and the ψ meson.

In a recent paper [1] this nontrivial problem was formally solved by first assuming a *general* flow velocity profile $\mathbf{v}(x)$ and thereafter deriving new statistical mechanical expressions for the gluon number density $n_g(x)$, the average dissociation rate $\langle\tilde{\Gamma}(x)\rangle$, and the ψ meson survival probability $S(p_{\mathrm{T}})$ at transverse momentum p_{T} (assuming the meson's velocity $\mathbf{v}_\psi$ to be along the lateral X direction in the fireball frame).

This general theory was also applied numerically in [1] to a plasma undergoing a pure *longitudinal* expansion parallel to the collision axis. In such a case the kinematics is simple because $\mathbf{v}\cdot\mathbf{v}_\psi = 0$ and also the cooling is known [9] to occur slowly. When a comparison was made with the no-flow situation [8] we found that $n_g(x)$ was enhanced, a partial-wave interference mechanism operated in $\langle\tilde{\Gamma}(x)\rangle$, and the graph of $S(p_{\mathrm{T}})$ was pushed down/up depending on the LHC/RHIC initial conditions.

The aim of the present paper is to address the following important question [9]: What will happen if the general theory of [1] is applied to the case of cylindrically symmetric, pure transverse expansion involving tougher kinematics (because $\mathbf{v}\cdot\mathbf{v}_\psi \neq 0$) as well as a higher cooling rate? In Sect. 2 below we derive the relevant formulae for statistical observables (viz. n_g, $\langle\tilde{\Gamma}\rangle$, $S(p_{\mathrm{T}})$, etc.) paying careful attention to the ψ meson trajectory and the so called catch-up time. Next, Sect. 3 presents our detailed numerical work along with interpretations concerning $\langle\tilde{\Gamma}\rangle$ and $S(p_{\mathrm{T}})$. Finally, our main conclusions are summarized in Sect. 4.

2 Statistical observables

2.1 Hydrodynamic aspects

We assume local thermal equilibrium and set up a *cylindrical* coordinate system in the fireball frame appropriate to a central collision. Let $\mathbf{x} = (r, \phi, z)$ be a typical spatial point, $x^\mu = (t, \mathbf{x})$ a time-space point, $\mathbf{v}$ the fluid three velocity, $\gamma = \left(1 - v^2\right)^{-1/2}$ the Lorentz factor, τ the proper time, $u^\mu = (\gamma, \gamma\mathbf{v})$ the four velocity, P the comoving pressure,

[a] e-mail: binoyfph@iitr.ernet.in

ϵ the comoving energy density, T the temperature, and $T^{\mu\nu} = (\epsilon + P)\, u^\mu u^\nu - P g^{\mu\nu}$ the energy-momentum tensor. Then the expansion of the system is described by the equation for conservation of energy and momentum of an ideal fluid:

$$\partial_\mu T^{\mu\nu} = 0\,, \tag{1}$$

in conjunction with the equation of state for a partially equilibrated plasma of massless particles:

$$\epsilon = 3P = \left[a_2 \lambda_g + b_2(\lambda_q + \lambda_{\bar{q}})\right] T^4\,, \tag{2}$$

where $a_2 = 8\pi^2/15$, $b_2 = 7\pi^2 N_f/40$, and $N_f \approx 2.5$ is the number of dynamical quark flavors, λ_g is the gluon fugacity, and $\lambda_{\bar{q}}$ (λ_q) is the (anti-) quark fugacity. Of course, the gluons (or quarks) obey Bose–Einstein (or Fermi–Dirac) statistics having fugacities λ_g (or λ_q) at temperature T.

The number densities of massless quarks and gluons are known to be proportional to T^3 where T is the local temperature as a function of the medium's proper time τ. As the plasma expands in the fireball frame, cooling occurs, i.e., T decreases with the clock time t at every spatial location $\mathbf{x}$. The law of decrease of T is like $\tau^{-1/3}$ for a pure longitudinal flow (as predicted by Bjorken's boost-invariant theory) but is more rapid for a pure transverse flow (as shown by numerical computations). Therefore, expansion necessarily causes a *dilution* of the system's density as the time progresses.

Under transverse expansion the fugacities and temperature evolve with the proper time according to the master rate equations [10–12]

$$\begin{aligned}
&\frac{\gamma}{\lambda_g}\partial_t \lambda_g + \frac{\gamma v}{\lambda_g}\partial_r \lambda_g + \frac{1}{T^3}\partial_t(\gamma T^3) + \frac{v}{T^3}\partial_r(\gamma T^3) \\
&\quad + \gamma \partial_r v + \gamma\left(\frac{v}{r} + \frac{1}{t}\right) \\
&= R_3(1-\lambda_g) - 2R_2\left(1 - \frac{\lambda_q \lambda_{\bar{q}}}{\lambda_g^2}\right)\,,
\end{aligned} \tag{3}$$

$$\begin{aligned}
&\frac{\gamma}{\lambda_q}\partial_t \lambda_q + \frac{\gamma v}{\lambda_q}\partial_r \lambda_q + \frac{1}{T^3}\partial_t(\gamma T^3) + \frac{v}{T^3}\partial_r(\gamma T^3) \\
&\quad + \gamma \partial_r v + \gamma\left(\frac{v}{r} + \frac{1}{t}\right) \\
&= R_2 \frac{a_1}{b_1}\left(\frac{\lambda_g}{\lambda_q} - \frac{\lambda_{\bar{q}}}{\lambda_g}\right)\,,
\end{aligned} \tag{4}$$

where v is the transverse velocity, and the remaining symbols are defined by

$$R_2 = 0.5 n_g \langle v_{\rm rel}\sigma_{gg\longrightarrow q\bar{q}}\rangle, \quad R_3 = 0.5 n_g \langle v_{\rm rel}\sigma_{gg\longrightarrow ggq}\rangle\,. \tag{5}$$

For our phenomenological purposes it will suffice to assume that, at a general instant t in the fireball frame, the plasma is contained in a uniformly expanding cylinder of radius

$$R = R_{\rm i} + (t - t_{\rm i})\, v_{\rm e}\,, \tag{6}$$

where $R_{\rm i}$ was the radius at the initial instant $t_{\rm i}$ and the expansion speed $v_{\rm e}$ is a free parameter ($0 \le v_{\rm e} < 1$). In the absence of azimuthal rotations the transverse velocity profile of the medium can be parametrized by a linear ansatz:

$$\mathbf{v} = v_{\rm e}\, \mathbf{r}/R, \qquad 0 \le r \le R\,. \tag{7}$$

Clearly, $|\mathbf{v}|$ vanishes at the origin but becomes $v_{\rm e}$ at the edge. The (chemical) master equations (3)–(4) are designed to be solved numerically on a computer subject to the RHIC/LHC initial conditions stated in Table 1.

The lifetime or freeze-out time $t_{\rm life}$ of the plasma is the instant when the temperature at the edge falls to $T(t_{\rm life}) = 0.2$ GeV, say.

2.2 Gluon number density

For an *arbitrary* flow profile $\mathbf{v}$, momentum integration [1, Eq. 11] over a Bose–Einstein distribution function yields the evolving gluon number density

$$n_g(x) = \frac{16}{\pi^2}\,\gamma\, T^3 \sum_{n=1}^{\infty} \frac{\lambda_g^n}{n^3}\,. \tag{8}$$

It may appear to be counterintuitive that the density of gluons should increase in the expansion; however, a simple physical explanation is offered by the concept of length (or volume) contraction in Lorentz transformations. Suppose a given number N_g^0 of gluons are present in a small volume V_g^0 which is locally at rest with respect to the plasma; the corresponding density $n_g^0 = N_g^0/V_g^0$ may be called *proper*. Upon making a Lorentz boost with velocity $-\mathbf{v}$ the new observer (in the fireball frame) sees the same number of gluons within a contracted volume $V_g = V_g^0/\gamma$; the corresponding density $n_g = N_g^0/V_g = n_g^0\gamma$ therefore becomes enhanced in (8).

Of course, the issue of a volume contraction between two frames is based on the hypothesis of temporal *simultaneity* in each, and this issue is quite different from the

Table 1. Colliding nuclei, collision energy, and initial parameters for the QGP at RHIC(1), LHC(1) [13]

	Nuclei	Energy $\sqrt{s}$ (GeV/nucleon)	$t_{\rm i}$ (fm/c)	$T_{\rm i}$ (GeV)	$\lambda_{g{\rm i}}$	$\lambda_{q{\rm i}}$	$R_{\rm i}$ (fm)
RHIC(1)	^{197}Au	200	0.7	0.55	0.05	0.008	6.98
LHC(1)	^{208}Pb	5000	0.5	0.82	0.124	0.02	7.01

question of the time-evolution of the gluon number density in a given frame. Indeed, at a specified location $\mathbf{x}$ in the fireball frame our n_g will steadily decrease with time as the expansion (i.e. cooling) proceeds due to the T^3 factor in (8).

Since this expression does not depend on the angles of $\mathbf{v}$ it has the same structure both for the longitudinal and transverse cases. Also, the flow *enhances* the number density compared to the no-flow case [8]; e.g. at fixed λ_g the enhancement factor γ becomes 2.3 if $|\mathbf{v}| = 0.9c$.

2.3 Average ψ dissociation rate

In the fireball frame (keeping the flow profile still general) we consider a ψ meson of mass m_ψ, four momentum p^μ_ψ, three velocity $\mathbf{v}_\psi = \mathbf{p}_\psi/p^0_\psi$, and Lorentz factor $\gamma_\psi = p^0_\psi/m_\psi$. If w^μ is the plasma four velocity measured in the *rest frame* of ψ then we can define the useful kinematic symbols [1, Eq. 30]

$$\begin{aligned} F &= \mathbf{v}\cdot\hat{v}_\psi, \qquad Y = \gamma_\psi|\mathbf{v}_\psi| - (\gamma_\psi - 1)\,F, \\ w^0 &= \gamma\gamma_\psi\,(1 - F|\mathbf{v}_\psi|)\,, \qquad \mathbf{w} = \gamma\,(\mathbf{v} - Y\hat{v}_\psi)\,, \\ \cos\theta_{\psi w} &= \hat{w}\cdot\hat{v}_\psi = \gamma\,(F - Y)\,/|\mathbf{w}|\,, \end{aligned} \tag{9}$$

where the hats stand for unit vectors. Now, let q^μ be the gluon four momentum seen in the ψ meson rest frame, ϵ_ψ the $c\bar{c}$ binding energy, $Q^0 = q^0/\epsilon_\psi$ a dimensionless variable, and $\sigma_{\mathrm{Rest}}(Q^0) \propto \left(Q^0 - 1\right)^{3/2}/Q^{0\,5}$ the g–ψ breakup cross section according to QCD [14]. Then the mean dissociation rate due to hard thermal gluons [1, Eq. 32] is given by

$$\begin{aligned} \langle\tilde{\Gamma}(x)\rangle = \frac{8\epsilon^3_\psi\gamma_\psi}{\pi^2}\sum_{n=1}^{\infty}\lambda^n_g\int_1^\infty \mathrm{d}Q^0 Q^{0\,2}\sigma_{\mathrm{Rest}}(Q^0)\mathrm{e}^{-C_n Q^0} \\ \times\left[I_0(\rho_n) + I_1(\rho_n)|\mathbf{v}_\psi|\cos\theta_{\psi w}\right]\,, \end{aligned} \tag{10}$$

where we have used the abbreviations

$$\begin{aligned} C_n &= n\epsilon_\psi w^0/T, \qquad D_n = n\epsilon_\psi|\mathbf{w}|/T, \\ \rho_n &= D_n Q^0, \qquad I_0(\rho_n) = \sinh(\rho_n)/\rho_n, \\ I_1(\rho_n) &= \cosh(\rho_n)/\rho_n - \sinh(\rho_n)/\rho^2_n.\,. \end{aligned} \tag{11}$$

Equation (10) demonstrates how $\langle\tilde{\Gamma}(x)\rangle$ depends on the hydrodynamic flow through w^μ as well as the angle $\theta_{\psi w}$. Retaining only the $n=1$ term and picking up the dominant peak contribution from $Q^0_p = 10/7$ we arrive at the useful approximation

$$\begin{aligned} &\langle\tilde{\Gamma}(x)\rangle \propto \lambda_g\gamma_\psi H, \\ &H \equiv \mathrm{e}^{-C_1 Q^0_p}\left[I_0(D_1 Q^0_p) + I_1(D_1 Q^0_p)\mid\mathbf{v}_\psi\mid\cos\theta_{\psi w}\right]\,, \end{aligned} \tag{12}$$

in which a partial-wave *interference* mechanism operates due to the anisotropic $\cos\theta_{\psi\omega}$ factor. Numerical consequences of (10) relevant to transverse flow will be discussed later in Sect. 3.1.

2.4 J/ψ survival probability

In this section we shall consider pure *transverse* flow parametrized by (7) and the ψ meson moving in the *lateral* X direction with velocity $\mathbf{v}_\psi = (v_{\mathrm{T}}, 0, 0)$ appropriate to the mid-rapidity region in the fireball frame. Suppressing the z coordinate the production configuration of the ψ meson is called $\left(t_{\mathrm{I}}, \mathbf{r}^{\mathrm{I}}_\psi\right) \equiv \left(t_{\mathrm{I}}, r^{\mathrm{I}}_\psi, \phi^{\mathrm{I}}_\psi\right)$ and the general trajectory after time duration Δ is termed $(t, \mathbf{r}_\psi) \equiv \left(t, r_\psi, \phi^{\mathrm{I}}_\psi\right)$ such that

$$\begin{aligned} t_{\mathrm{I}} &= t_{\mathrm{i}} + \gamma_\psi\tau_{\mathrm{F}}, \qquad \Delta = t - t_{\mathrm{I}} \\ \mathbf{r}_\psi &= \mathbf{r}^{\mathrm{I}}_\psi + \mathbf{v}_\psi\Delta\,, \end{aligned} \tag{13}$$

where $\tau_{\mathrm{F}} \approx 0.89\,\mathrm{fm}/c$ is the proper formation time [15] of the $c\bar{c}$ bound state. This transverse trajectory will hit the edge $R \equiv R_{\mathrm{I}} + v_{\mathrm{e}}\Delta$ of the radially expanding cylinder (cf. (6)) at the *catch-up* instant t^* after duration Δ^* such that

$$\begin{aligned} &\mid R_{\mathrm{I}} + v_{\mathrm{e}}\Delta^*\mid^2 = \mid\mathbf{r}^{\mathrm{I}}_\psi + \mathbf{v}_\psi\Delta^*\mid^2, \\ &\text{so}\quad \alpha\Delta^{*2} + 2\beta\Delta^* - \mu = 0, \\ &\text{with}\quad \alpha = v^2_\psi - v^2_{\mathrm{e}}, \qquad \mu = R^2_{\mathrm{I}} - r^{\mathrm{I}\,2}_\psi, \\ &\beta = r^{\mathrm{I}}_\psi v_\psi\cos\phi^{\mathrm{I}}_\psi - R_{\mathrm{I}}v_{\mathrm{e}}\,. \end{aligned} \tag{14}$$

If the quadratic equation in Δ^* has real roots we pick up the one which is positive and smaller; but if both roots are imaginary then a catch-up cannot occur. The time interval of physical interest becomes

$$t_{\mathrm{I}} \le t \le t_{\mathrm{II}}\,, \qquad t_{\mathrm{II}} = \min\left(t_{\mathrm{I}} + \Delta^*,\ t_{\mathrm{life}}\right)\,. \tag{15}$$

This formula is quite different from that derived in the case of longitudinal flow [1, Eq. 48]. As the time t progresses the dissociation rate (10) must be evaluated on the ψ meson trajectory itself, implying that we have to set at a general instant

$$\begin{aligned} &\mathbf{r} = \mathbf{r}_\psi, \qquad \mathbf{v} = v_{\mathrm{e}}\mathbf{r}_\psi/R, \\ &F \equiv \mathbf{v}\cdot\hat{v}_\psi = \left(\frac{v_{\mathrm{e}}}{R}\right)\left(r^{\mathrm{I}}_\psi\cos\phi^{\mathrm{I}}_\psi + v_\psi\Delta\right) \end{aligned} \tag{16}$$

in the kinematic relations (9). Clearly, the notation $\langle\tilde{\Gamma}\rangle$ of (10) becomes equivalent to

$$\langle\tilde{\Gamma}[t]\rangle \equiv \langle\tilde{\Gamma}(t, p_{\mathrm{T}}, r^{\mathrm{I}}_\psi, \phi^{\mathrm{I}}_\psi)\rangle, \tag{17}$$

depending parametrically on the production configuration r^{I}_ψ, ϕ^{I}_ψ. Then, by using the radioactive decay law without recombination and averaging over the cross sectional area $A_{\mathrm{I}} = \pi R^2_{\mathrm{I}}$ (at the production instant) we arrive at the desired survival probability:

$$\begin{aligned} S(p_{\mathrm{T}}) &= \int_{A_{\mathrm{I}}}\mathrm{d}^2r^{\mathrm{I}}_\psi\left(R^2_{\mathrm{I}} - r^{\mathrm{I}\,2}_\psi\right)\mathrm{e}^{-W}\Big/\int_{A_{\mathrm{I}}}\mathrm{d}^2r^{\mathrm{I}}_\psi\left(R^2_{\mathrm{I}} - r^{\mathrm{I}\,2}_\psi\right), \\ W &= \int_{t_{\mathrm{I}}}^{t_{\mathrm{II}}}\mathrm{d}t\ \tilde{\Gamma}[t]\,, \qquad \mathrm{d}^2r^{\mathrm{I}}_\psi = \mathrm{d}r^{\mathrm{I}}_\psi r^{\mathrm{I}}_\psi\mathrm{d}\phi^{\mathrm{I}}_\psi\,. \end{aligned} \tag{18}$$

To appreciate more fully the physics of (13)–(18) it is convenient to recapitulate briefly how J/Ψ production is modeled in the standard literature. In ultrarelativistic heavy ion collisions the gluonic content of the individual nucleon–nucleon interactions can create heavy quark–antiquark flavors over the very short time scale $\sim 1/2m_c \sim 10^{-24}$ s, with m_c being the mass of the charm quark. The $c\bar{c}$ pair traversing the deconfined medium develops into the physical Ψ resonance after a formation time. Although the transverse momentum $\mathbf{p}_\psi$ of the meson is selected experimentally, its transverse location $\mathbf{r}_\psi^{\mathrm{I}}$ at the instant of creation remains a *random* variable with a chance distribution $\Pi(r_\psi^{\mathrm{I}})$, say. Assuming that the creation rate of J/Ψ is proportional to the number of participant NN interactions at impact parameter r_ψ^{I} one finds $\Pi(r_\psi^{\mathrm{I}}) \propto (R_{\mathrm{I}}^2 - {r_\psi^{\mathrm{I}}}^2)$ which enters the basic formula (18). Clearly the distribution $\Pi(r_\psi^{\mathrm{I}})$ is *nonuniform*, because it is maximum at $r_\psi^{\mathrm{I}} = 0$ but vanishes at $r_\psi^{\mathrm{I}} = R_{\mathrm{I}}$.

Here no information is needed about the length L_{I} of the cylindrical plasma in contrast to the case of longitudinal flow [1, Eq. 52] where the averaging had to be done over the volume $V_{\mathrm{I}} = \pi R_{\mathrm{I}}^2 L_{\mathrm{I}}$.

3 Numerical results

3.1 Curves of dissociation rate

The exact formula (10) of $\langle\tilde{\Gamma}\rangle$ is a very complicated function of t as well as of several kinematic parameters defined jointly by (9), (11) and (16), but a feeling for its behavior can be obtained in the extreme nonrelativistic ($|\mathbf{v}|/c \to 0$) and ultrarelativistic ($|\mathbf{v}|/c \to 1$) limits. For simplicity, suppose at the *instant* t_I a special ψ was formed almost at the edge R_{I} of the cylinder with ϕ_ψ^{I} being the angle between the ψ position vector and the velocity vector. Then the kinematic relations (16) and (9) yield

$$\begin{aligned} \mathbf{v} &= v_{\mathrm{e}}\hat{r}_\psi^{\mathrm{I}} = \pm v_{\mathrm{e}}\hat{v}_\psi, \quad F = v_{\mathrm{e}}\cos\phi_\psi^{\mathrm{I}} = \pm v_{\mathrm{e}}, \\ \mathbf{w} &= \gamma\,(\mathbf{v} - Y\hat{v}_\psi) = \gamma_e\,(\pm v_{\mathrm{e}} - Y)\,\hat{v}_\psi\,, \end{aligned} \tag{19}$$

where the $+$, $-$ signs correspond to $\cos\phi_\psi^{\mathrm{I}} = \pm 1$, i.e., to $\phi_\psi^{\mathrm{I}} = 0, \pi$, respectively. Thus we have the parallel or antiparallel property

$$\begin{aligned} &\mathbf{w} \parallel \hat{v}_\psi, \quad \cos\phi_{\psi w} = +1 \text{ if } \phi_\psi^{\mathrm{I}} = 0 \text{ and } Y < v_{\mathrm{e}}, \\ &\mathbf{w} \parallel -\hat{v}_\psi, \quad \cos\phi_{\psi w} = -1 \text{ if } \phi_\psi^{\pm} = \pi \text{ or } Y > v_{\mathrm{e}}\,. \end{aligned} \tag{20}$$

Results for intermediate values of $\phi_{\psi w}$ will not be reported here. Figures 1–4 depict the corresponding exact curves of $\langle\tilde{\Gamma}\rangle$ computed from (10) based on the LHC initial conditions of Table 1 We now proceed to interpret these graphs using the approximate estimate (12).

Interpretation

i) At fixed $(p_{\mathrm{T}}, \phi_\psi^{\mathrm{I}}, v_{\mathrm{e}})$ the steady *increase* of $\langle\tilde{\Gamma}\rangle$ with T in Figs. 1–2 is caused by the growing $\exp\{-(C_1 \mp D_1)Q_p^0\}$ factors occurring in the estimate (12).

ii) At fixed value of $(T, \phi_\psi^{\mathrm{I}}, v_{\mathrm{e}} = 0.2)$ corresponding to a *nonrelativistic* flow the variation of $\langle\tilde{\Gamma}\rangle$ with p_{T} in Fig. 3a and b is more intricate. At $\phi_\psi^{\mathrm{I}} = 0$ in Fig. 3a there is a broad *enhancement* of $\langle\tilde{\Gamma}\rangle$ for low $p_{\mathrm{T}} \leq$ 1 GeV; this is because, firstly, low speeds of the ψ and plasma can compete, and, secondly, constructive interference occurs between I_0 and I_1 in the estimate (12) for $\cos\theta_{\psi w} = +1$ (cf. (20)). On the other hand, at $\phi_\psi^{\mathrm{I}} = \pi$ in Fig. 3b our $\langle\tilde{\Gamma}\rangle$ *decreases* monotonically with p_{T} throughout; this is due to the fact that, since $\cos\theta_{\psi w} = -1$ now (cf. (20)), the interference between I_0 and I_1 becomes destructive.

iii) At fixed values of $(T, \phi_\psi^{\mathrm{I}}, v_{\mathrm{e}} = 0.9)$ corresponding to an *ultrarelativistic* flow similar trends with respect to p_{T} are again explained in Fig. 4a and b, except for the fact that the steady *rise* of $\langle\tilde{\Gamma}\rangle$ with p_{T} in Fig. 4a is caused mainly by the γ_ψ coefficient present in the estimate (12).

3.2 Curves of survival probability

For a chosen creation configuration of the ψ meson the function W was first computed from (18) and then $S(p_{\mathrm{T}})$ was numerically evaluated. Figure 5a and b show the dependence of $S(p_{\mathrm{T}})$ on p_{T} corresponding to the LHC and RHIC initial conditions, respectively (for two choices of the transverse expansion speed v_{e}). For the sake of a direct comparison, we also include our earlier results based on no-flow [8, Eq. 25] and longitudinal expansion [1, Eq. 52] (starting from two possible lengths L_{i} of the initial cylinder). We now turn to a physical discussion of these graphs.

Interpretation

In every scenario of gluonic dissociation the function $W = \int_{t_{\mathrm{I}}}^{t_{\mathrm{II}}} \mathrm{d}t\,\langle\tilde{\Gamma}\rangle$ depends on p_{T} via the integrand $\langle\tilde{\Gamma}\rangle$ as well as the limits $(t_{\mathrm{I}}, t_{\mathrm{II}})$. Three interesting cases may now be distinguished.

No flow case. Here [8] cooling of the plasma is simulated through the master rate equations [10], but the existence of the explicit flow profile is ignored. Then $\langle\tilde{\Gamma}\rangle$ decreases monotonically with p_{T} because of a destructive interference between the I_0 and I_1 terms. Also, the time span $t_{\mathrm{II}} - t_{\mathrm{I}}$ is shortened as the speed of the ψ meson increases. Consequently, the survival probability called $S_0(p_{\mathrm{T}})$ grows steadily with p_{T} as shown by the solid lines in Fig. 5a and b.

Longitudinal expansion case. Here [1] an extra parameter appears, namely the length L_{i} of the initial cylinder. For nonrelativistic flow emanating from the short length of $L_{\mathrm{i}} = 0.1$ fm, the $\langle\tilde{\Gamma}\rangle$ values are somewhat reduced compared to the no-flow case (due to I_0, I_1 destructive interference), though the time span $t_{\mathrm{II}} - t_{\mathrm{I}}$ remains unaltered, so that the survival probability, called $S_\parallel(p_{\mathrm{T}})$, is pushed slightly upwards in Fig. 5a and b. But for relativistic flow

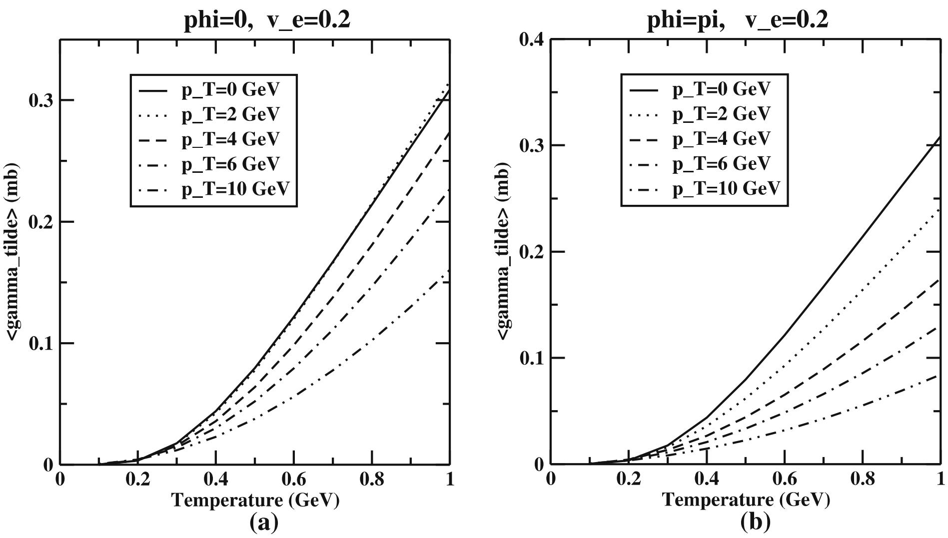

Fig. 1. The variation of the modified rate $\langle\tilde{\Gamma}\rangle$ as a function of temperature at different transverse momenta for the transverse flow velocity $v = 0.2c$ for **a** $\phi_\psi^{\mathrm{I}} = 0$ and **b** $\phi_\psi^{\mathrm{I}} = \pi$, respectively

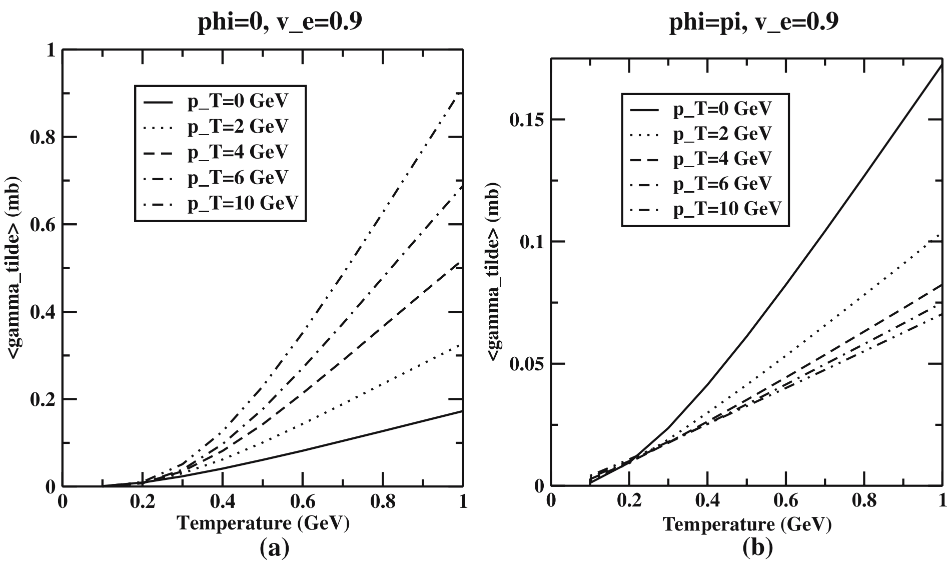

Fig. 2. The variation of the modified rate $\langle\tilde{\Gamma}\rangle$ as a function of temperature at different transverse momenta for the transverse flow velocity $v = 0.9c$ for **a** $\phi_\psi^{\mathrm{I}} = 0$ and **b** $\phi_\psi^{\mathrm{I}} = \pi$, respectively

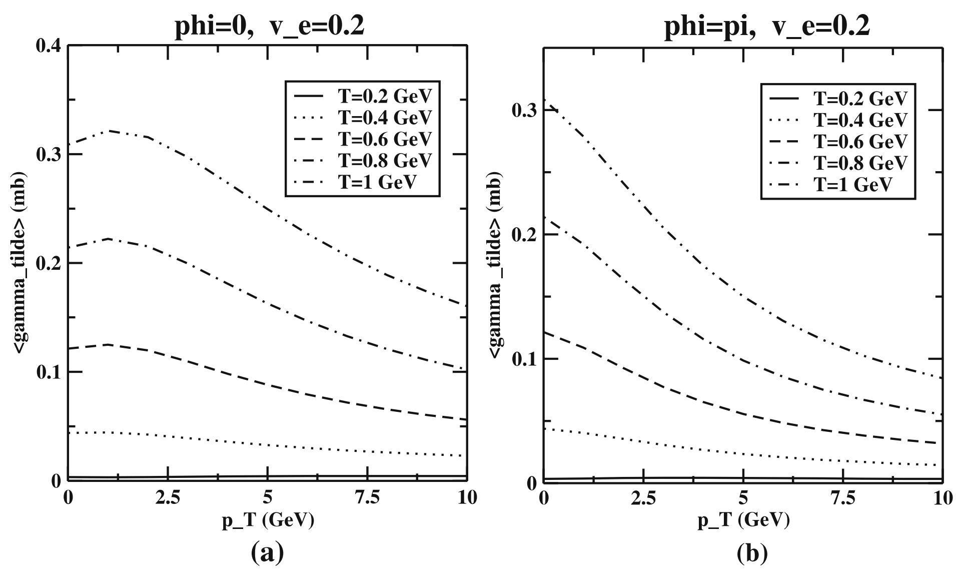

Fig. 3. The variation of the modified rate $\langle\tilde{\Gamma}\rangle$ as a function of transverse momentum for different values of temperatures for the transverse flow velocity $v = 0.2c$ for **a** $\phi_\psi^{\mathrm{I}} = 0$ and **b** $\phi_\psi^{\mathrm{I}} = \pi$, respectively

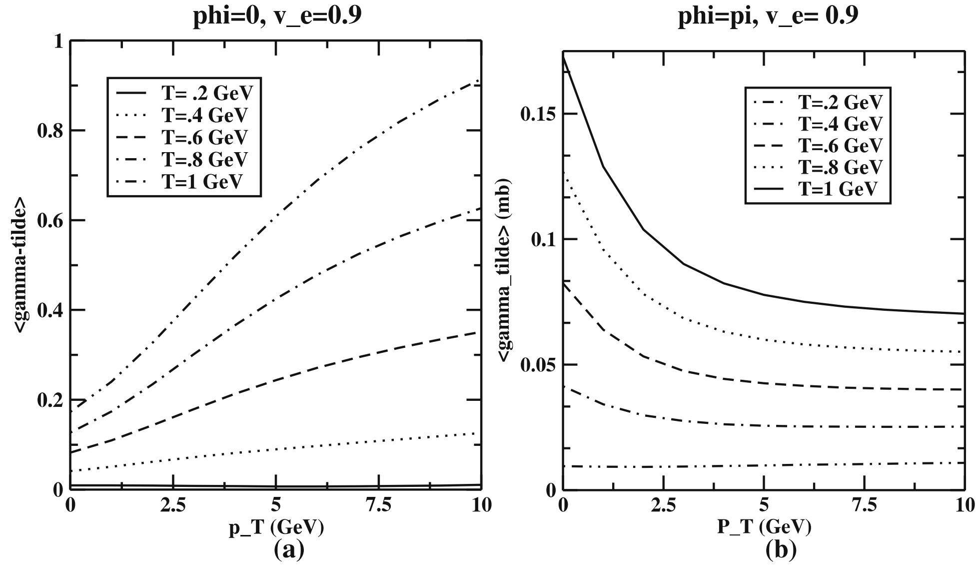

Fig. 4. The variation of the modified rate $\langle\tilde{\Gamma}\rangle$ as a function of transverse momentum at different values of the temperature for the transverse flow velocity $v = 0.9c$ for **a** $\phi_\psi^{\mathrm{I}} = 0$ and **b** $\phi_\psi^{\mathrm{I}} = \pi$, respectively

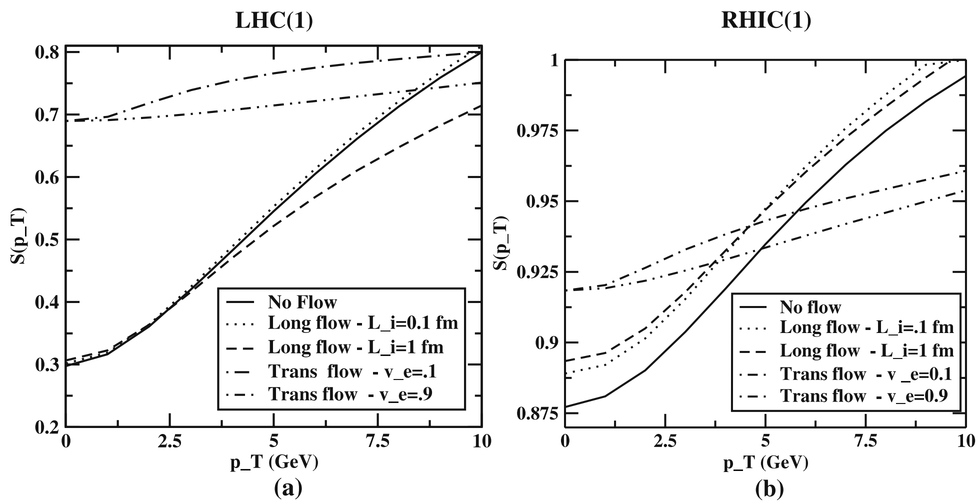

Fig. 5. The survival probability of J/ψ in an equilibrating parton plasma at **a** LHC(1) and **b** RHIC(1) energies with initial conditions given in Table 1. The *solid curve* $S_0(p_\mathrm{T})$ is the result of [8], i.e., in the *absence of flow*, while the *dotted* and *dashed curves* represent the $S_\parallel(p_\mathrm{T})$ when the plasma is undergoing longitudinal expansion with the initial values of the length of the cylinder $L_\mathrm{i} = 0.1$ fm and 1 fm, respectively [1]. The *dot-dashed* and *double dot-dashed curves* depict the $S_\perp(p_\mathrm{T})$ when the system is undergoing a transverse expansion with the expansion speed $v_\mathrm{e} = 0.1$ and 0.9, respectively

emanating from the longer length of $L_\mathrm{i} = 1$ fm the shifts of the $S_\parallel(p_\mathrm{T})$ curve occurs in mutually opposite directions at LHC and RHIC (due to the different initial temperatures generated therein [1]).

Transverse expansion case. Here the extra parameter involved is the transverse expansion speed v_e which together with ϕ_ψ^{I} and T control the p_T-dependence of the function W. For $\phi_\psi^{\mathrm{I}} = 0$ the $\langle\tilde{\Gamma}\rangle$ values in Figs. 3a and 4a exhibit an enhancement/rising trend on the lower p_T side; such ψ mesons contribute sizably to W but little to e^{-W}. On the other hand, all curves of $\langle\tilde{\Gamma}\rangle$ in Figs. 3 and 4 flatten off to nearly constant values on the higher p_T side; such ψ mesons contribute substantially to e^{-W} especially for low temperatures. Therefore, the transverse survival probability $S_\perp(p_\mathrm{T})$ becomes nearly p_T-independent (or very slowly varying) in Fig. 5a and b, in sharp contrast to the longitudinal case. For explaining the magnitude of the ratio $S_\perp(p_\mathrm{T})/S_\parallel(p_\mathrm{T})$ we consider the temporal scenario dealing with the limits of the integration.

Temporal scenario. It is known that a transverse expansion of a quark–gluon plasma produces cooling at a faster rate compared to longitudinal expansion, so that the inequality $t_{\mathrm{life}}^{\perp} < t_{\mathrm{life}}^{\parallel}$ holds on the corresponding lifetimes. At LHC the transverse cooling is so fast that for most ψ mesons of kinematic interest we have $t_{\mathrm{II}} = t_{\mathrm{life}}^{\perp}$ in the definition (15). The time span $t_{\mathrm{II}} - t_{\mathrm{I}}$ is, therefore, much smaller compared to the longitudinal case implying $S_\perp(p_\mathrm{T}) > S_\parallel(p_\mathrm{T})$ in Fig. 5a. Clearly this property at LHC is devoid of any rich structure. However, at RHIC let us divide the ψ meson kinematic region into two parts. For slower mesons having $p_\mathrm{T} < 5$ GeV the catch-up time $t_\mathrm{I} + \Delta^*$ in (15) exceeds the lifetime so that $t_{\mathrm{II}} = t_{\mathrm{life}}^{\perp}$ again, i.e., $S_\perp(p_\mathrm{T}) > S_\parallel(p_\mathrm{T})$ in Fig. 5b for $p_\mathrm{T} < 5$ GeV. Next, for faster mesons having $p_\mathrm{T} > 5$ GeV, the reverse inequalities hold, making $S_\perp(p_\mathrm{T}) < S_\parallel(p_\mathrm{T})$ in Fig. 5b. Clearly, the rich structure in $S_\perp(p_\mathrm{T})$ at RHIC arises from a mutual competition between the catch-up time and the lifetime.

One may still wonder what will happen in the more *realistic* situation where the longitudinal and transverse expansions occur simultaneously. It is difficult to give a concrete quantitative answer to this question due to two-fold reasons.

i) In the cylindrical coordinates the full form of the hydrodynamical equation (1) and master rate equations becomes too tedious even for a computer, and
ii) the kinematic relations (9) describing the flow in J/Ψ rest frame also become complicated since $\mathbf{v}$ is a full-fledged three vector.

Hence we content ourselves with the qualitative remark that the realistic curves of $S(p_{\mathrm{T}})$ will presumably lie in between those for the pure longitudinal flow and pure transverse flow shown in Fig. 5.

4 Conclusions

a) In this work we have applied our general formulation [1] of the hydrodynamic expansion to study the effect of an explicit transverse flow profile on the gluonic breakup of J/ψs created in an equilibrating QGP. The formalism in Sect. 2 and numerical results of Sect. 3 are new and original.
b) Equation (8) shows that, at specified fugacity λ_g, the effect of the transverse flow is to increase the gluon number density n_g. This was also the case with longitudinal flow.
c) Our expressions (10) and (12) of the mean dissociation rate $\langle\tilde{\Gamma}\rangle$ involves hyperbolic functions as well as a partial-wave interference mechanism (controlled by the anisotropic $\cos\theta_{\psi w}$ factor). In addition, knowledge of a nontrivial kinematic function F (cf. (16)) is needed for interpreting the variation of $\langle\tilde{\Gamma}\rangle$ with T, p_{T}, ϕ_{ψ}^{I}, v_{e} in Figs. 1–4. In contrast, for longitudinal flow the treatment of $\langle\tilde{\Gamma}\rangle$ was easier because $F=0$ there.
d) There are several features of contrast between the transverse and longitudinal survival probabilities denoted by $S_{\perp}(p_{\mathrm{T}})$ and $S_{\parallel}(p_{\mathrm{T}})$, respectively. Due to the geometry of the production configuration our $S_{\perp}(p_{\mathrm{T}})$ contains a double integral (18) whereas $S_{\parallel}(p_{\mathrm{T}})$ contains a triple integral. Next, due to the flattening-off trend of $\langle\tilde{\Gamma}\rangle$ with increasing p_{T}, our $S_{\perp}(p_{\mathrm{T}})$ becomes roughly p_{T}-independent (or slowly varying) in Fig. 5a and b, whereas $S_{\parallel}(p_{\mathrm{T}})$ rises rapidly. Finally, the quick cooling rate at LHC makes $S_{\perp}(p_{\mathrm{T}}) > S_{\parallel}(p_{\mathrm{T}})$ at all p_{T} of interest in Fig. 5a whereas at RHIC (in Fig. 5b) a competition between the catch-up time and the lifetime will add to the richness of the information likely to be available from such studies. Of course a full study will additionally have to include the effect of the nuclear and the co-mover absorption, before comparing these interesting results with the experimental data.
e) We conclude with the observation that the field of J/ψ suppression due to gluonic breakup continues to be a research area of great challenge. In a future communication we plan to study the effect of an asymmetric flow profile arising from noncentral collisions of heavy ions at finite impact parameter $\mathbf{b}$.

Acknowledgements. VJM thanks the UGC, Government of India, New Delhi for financial support. We are also thankful to Dr. Dinesh Kumar Srivastava for discussions in the early stages of this work.

References

1. B.K. Patra, V.J. Menon, Eur. Phys. J. C **44**, 567 (2005)
2. H. Satz, Rept. Prog. Phys. **63**, 1511 (2000)
3. D. Kharzeev, H. Satz, Phys. Lett. B **334**, 155 (1994)
4. D. Kharzeev, H. Satz, Phys. Lett. B **366**, 316 (1996)
5. B.K. Patra, V.J. Menon, Nucl. Phys. A **708**, 353 (2002)
6. X.-M. Xu, D. Kharzeev, H. Satz, X.-N. Wang, Phys. Rev. C **53**, 3051 (1996)
7. B.K. Patra, D.K. Srivastava, Phys. Lett. B **505**, 113 (2001)
8. B.K. Patra, V.J. Menon, Eur. Phys. J. C **37**, 115 (2004)
9. D. Pal, B.K. Patra, D.K. Srivastava, Eur. Phys. J. C **17**, 179 (2000)
10. T.S. Biro, E. van Doorn, M.H. Thoma, B. Müller, X.-N. Wang, Phys. Rev. C **48**, 1275 (1993)
11. D.K. Srivastava, M.G. Mustafa, B. Müller, Phys. Rev. C **56**, 1064 (1997); Phys. Lett. B **396**, 45 (1997)
12. B.K. Patra, J. Alam, P. Roy, S. Sarkar, B. Sinha, Nucl. Phys. A **709**, 440 (2002)
13. X.-N Wang, M. Gyulassy, Phys. Rev. D **44**, 3501 (1991)
14. M.E. Peskin, Nucl. Phys. B **156**, 365 (1979); G. Bhanot, M.E. Peskin, Nucl. Phys. B **156**, 391 (1979)
15. F. Karsch, H. Satz, Z. Phys. C **51**, 209 (1991); F. Karsch, M.T. Mehr, H. Satz, Z. Phys. C **37**, 617 (1988)